ISSN 1064-2269, Journal of Communications Technology and Electronics, 2016, Vol. 61, No. 8, pp. 887–893. © Pleiades Publishing, Inc., 2016.
Original Russian Text © A.P. Anyutin, I.P. Korshunov, A.D. Shatrov, 2016, published in Radiotekhnika i Elektronika, 2016, Vol. 61, No. 8, pp. 757–764.

ON THE 60th ANNIVERSARY OF THE JOURNAL OF COMMUNICATIONS TECHNOLOGY AND ELECTRONICS

Plasmon Resonances in a Quartz Nanofilament Covered with Gold of Variable Thickness

A. P. Anyutin, I. P. Korshunov, and A. D. Shatrov

Fryazino Branch, Institute of Radio-Engineering and Electronics, Russian Academy of Sciences, pl. Vvedenskogo 1, Fryazino, Moscow oblast, 141190 Russia

e-mail: korip@ms.ire.rssi.ru

Received December 4, 2015

Abstract—A two dimensional problem of diffraction of a plane electromagnetic wave by a cylindrical gold shell is considered in the case when the boundaries of the shell are circular cylinders with displaced centers. The influence of the excentricity of the boundaries on the properties of plasmon resonances in the optical band is studied. The near and far fields and scattering spectra are calculated by rigorous methods. It is found that the excentricity of shell's boundaries gives rise to additional resonances. Analytical theory of scattering for thin shells is developed in the quasi-static approximation. It is shown that, in this case, the scattering and absorption spectra essentially depend on the displacement of the centers of the cylindrical boundaries but are independent of the direction of this displacement.

DOI: 10.1134/S1064226916080015

INTRODUCTION

Due to plasmon resonances, nanowires of noble metals are employed as sensors in the optical band [1]. In [2, 3], the properties of plasmon resonances in coaxial silver and gold nanotubes were studied. The aim of the present work is to study the specificities of plasmon resonances in noncoaxial gold nanoshells.

1. PROBLEM STATEMENT

Let us consider a two-dimensional problem of diffraction of a plane linearly polarized electromagnetic wave by a nanofilament covered with a gold layer of variable thickness (Fig. 1). Let a plane wave propagate in free space in the direction of the unit vector $(\cos\varphi_0, \sin\varphi_0, 0)$ and be characterized by the following components of the electromagnetic field:

$$\begin{aligned} H_z^0 &= \exp(-ikx\cos\varphi_0 - iky\sin\varphi_0),\\ E_x^0 &= -\eta\sin\varphi_0\exp(-ikx\cos\varphi_0 - iky\sin\varphi_0),\\ E_y^0 &= \eta\cos\varphi_0\exp(-ikx\cos\varphi_0 - iky\sin\varphi_0). \end{aligned} \quad (1)$$

The time dependence is chosen in the form of the factor $\exp(i\omega t)$, where $\omega = kc$, $k = 2\pi/\lambda$, c is the speed of light in vacuum, λ is the wavelength, and $\eta = \sqrt{\mu_0/\varepsilon_0} = 120\pi\ \Omega$ is the characteristic impedance of vacuum.

Gold fills a shell the boundaries of which are circular cylinders

$$\begin{aligned} x^2 + y^2 &= a^2,\\ (x+\delta)^2 + y^2 &= b^2, \end{aligned} \quad (2)$$

where a is the radius of the quartz filament and b is the outer radius of the structure. The centers of the outer and inner boundaries of the shell are displaced by a distance δ.

The spatial distribution of the permittivity in the structure under consideration is defined by the formula

$$\varepsilon(x,y) = \begin{cases} \varepsilon_{qz},\ x^2 + y^2 < a^2,\\ \varepsilon,\ x^2 + y^2 > a^2,\\ (x+\delta)^2 + y^2 < b^2,\\ 1,\ (x+\delta)^2 + y^2 > b^2, \end{cases} \quad (3)$$

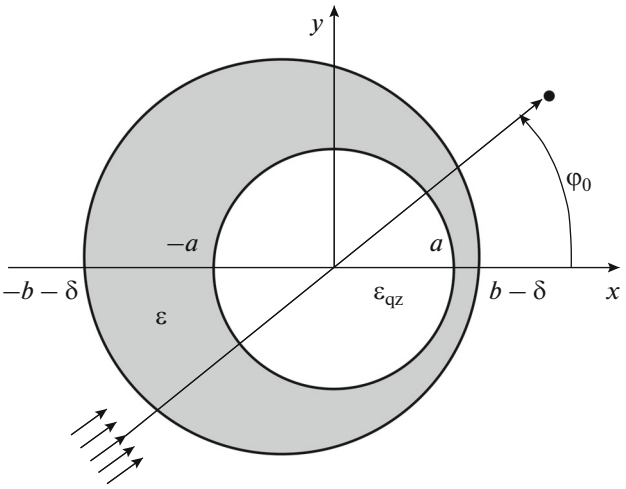

Fig. 1. Geometry of the problem.

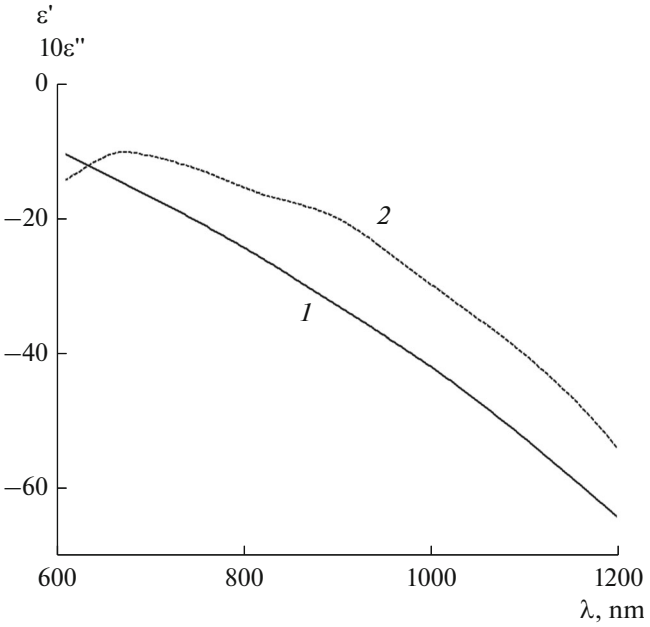

Fig. 2. The (*1*) real part ε' and (*2*) the imaginary part 10 ε" of the permittivity of gold vs. the wavelength.

where ε_{qz} and ε are the permittivities of quartz and gold, respectively.

We approximate the real and imaginary parts of the permittivity of gold, $\varepsilon = \varepsilon' + i\varepsilon''$, in the range $600 < \lambda < 1100$ nm by the functions presented in Fig. 2. The graphs of the functions were obtained by the interpolation of experimental data [4] by cubic splines.

Unlike gold, quartz in the same range has a substantially lower heat loss and its permittivity weakly depends on λ. Therefore, we assume the permittivity of quartz a real constant $\varepsilon_{qz} = 2.1$.

The analysis of the above-formulated diffraction problem is conveniently performed through the *z*-component of the magnetic field: $U(x, y) = H_z(x, y)$, because, in this case, the function $U(x, y)$ is scalar. Then, the components of the electric field can be expressed via the function $U(x, y)$ by the formulas

$$E_x(x,y) = \frac{\eta}{ik\varepsilon(x,y)}\frac{\partial U(x,y)}{\partial y}, \quad E_y(x,y) = \frac{-\eta}{ik\varepsilon(x,y)}\frac{\partial U(x,y)}{\partial x}, \tag{4}$$

and the total field satisfies the Helmholtz equation

$$\left[\frac{\partial^2}{\partial x^2} + \frac{\partial^2}{\partial y^2} + k^2\varepsilon(x,y)\right]U(x,y) = 0. \tag{5}$$

On the shell's boundaries, the quantities $U(x, y)$ and $\frac{1}{\varepsilon(x,y)}\frac{\partial U(x,y)}{\partial N}$ (N is the normal to the boundary) must be continuous.

The field outside the structure consists of the incident field U^0 and the scattered field U^s:

$$U = U^0 + U^s. \tag{6}$$

In the cylindrical coordinates ($x = r\cos\varphi$, $y = r\sin\varphi$), the incident field is defined by the function

$$U^0 = \exp[-ikr\cos(\varphi - \varphi_0)]. \tag{7}$$

The scattered field in the far zone must satisfy the radiation condition

$$U^s \sim \Phi(\varphi)\sqrt{\frac{2}{\pi kr}}\exp\left(-ikr + i\frac{\pi}{4}\right), \quad kr \to \infty, \tag{8}$$

where $\Phi(\varphi)$ is the far-field pattern.

The total scattering cross section σ_s is defined as

$$\sigma_s = \frac{2}{\pi k}\int_0^{2\pi} |\Phi(\varphi)|^2\, d\varphi. \tag{9}$$

The absorption cross section σ_a can be represented by the following integral over the outer contour of shell's boundary:

$$\sigma_a = \frac{1}{k}\,\mathrm{Im}\oint \frac{\partial U}{\partial N}U^*\, ds. \tag{10}$$

2. NUMERICA RESULTS

The numerical solution of the above-formulated problem was performed by the modified discrete sources method [5–7].

Figure 3 shows the total scattering cross sections as a function of the wavelength λ for the structures with fixed radii of the cylindrical shell's boundaries, $a = 45$ nm and $b = 50$ nm, and different distances between the centers of these boundaries. We see that, in the axisymmetic case ($\delta = 0$), there is a unique resonance and, with an increase in δ, additional resonances appear.

Figure 4 shows the distribution of the absolute value of the field $|U|$ along the outer boundary of the shell at the wavelength $\lambda = 810$ nm for the structure with the parameters $a = 45$ nm, $b = 50$ nm, and $\delta = 4.9$ nm (curve *1*). We see that, in the region where the shell is thinner ($\psi \approx 0$), oscillations are more frequent. This effect can be explained by the fact that the thin gold layer between two dielectric half-spaces maintains a strongly decelerated surface wave whose propagation constant increases with decreasing layer thickness. For comparison, the same figure presents the axisymmetric case ($\delta = 0$), when the thickness of the shell is independent of the angle ψ (curve *2*).

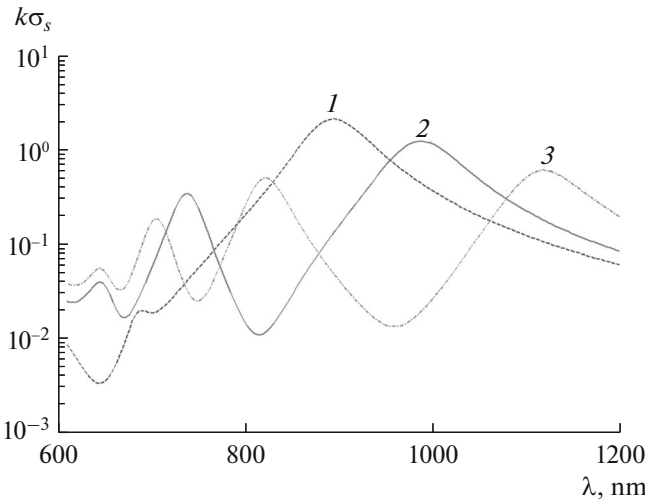

Fig. 3. The total scattering cross section vs. the wavelength for $a = 45$ nm, $b = 50$ nm, $\varphi_0 = 0$, and $\delta = (1)$ 0, (2) 3, and (3) 4 nm.

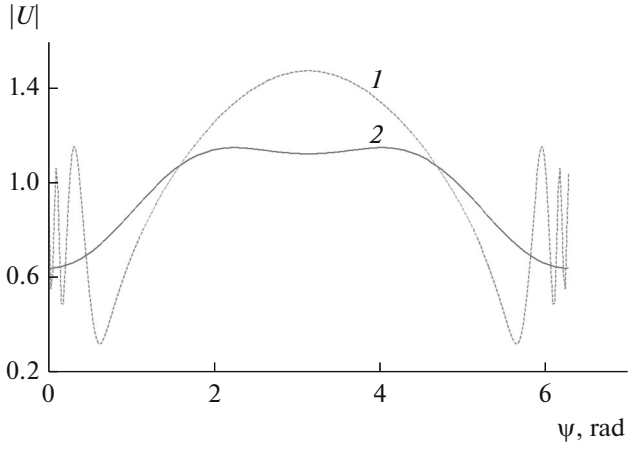

Fig. 4. The absolute value $|U(x, y)|$ of the field on the outer boundary of the shell vs. the angular coordinate ψ ($x = b\cos\psi - \delta$, $y = b\sin\psi$) for $a = 45$ nm, $b = 50$ nm, $\varphi_0 = 0$, $\lambda = 810$ nm, and $\delta = (1)$ 4.9 nm and (2) 0.

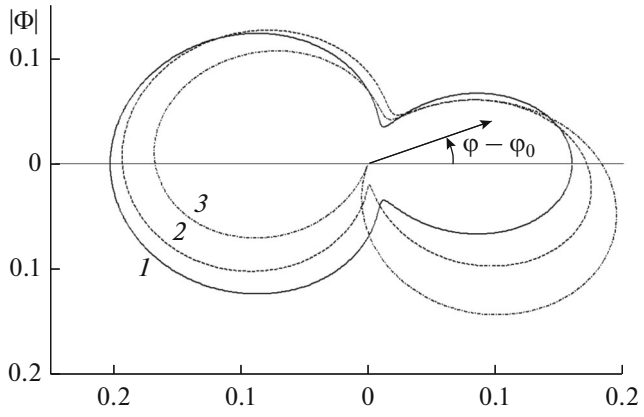

Fig. 5. The absolute values of the far-field patterns for $a = 45$ nm, $b = 50$ nm, $\delta = 4.8$ nm, $\lambda = 810$ nm, and $\varphi_0 = (1)$ 0, (2) π/4, and (3) π/2.

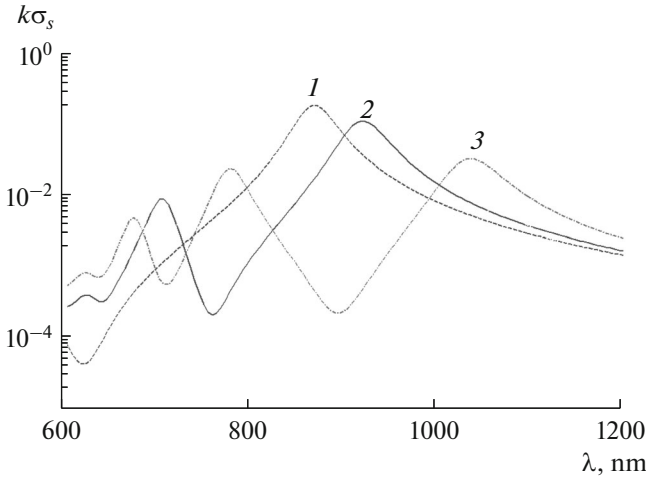

Fig. 6. The total scattering cross section of a shell vs. the wavelength for $a = 18$ nm, $b = 20$ nm, $\varphi_0 = 0$, and $\delta = (1)$ 0, (2) 1, and (3) 1.5 nm.

Figure 5 shows the far-field patterns $|\Phi(\varphi)|$ of the structure with the parameters $a = 45$ nm, $b = 50$ nm, and $\delta = 4.8$ nm at the wavelength $\lambda = 810$ nm for three different angles of incidence φ_0 of the plane wave. From the results presented in this figure, it follows that, regardless of the angle φ_0, the lobes of the far-field pattern $\Phi(\varphi)$ are approximately oriented in the direction of propagation of the plane wave ($\varphi = \varphi_0$) and in the opposite direction ($\varphi = \varphi_0 + \pi$).

Figures 6 and 7 illustrate the scattering properties of a smaller structure with the sizes $a = 18$ nm and $b = 20$ nm. These patterns are qualitatively close to Figs. 3 and 5. We notice that the far-field patterns presented in Fig. 7 depend with a high accuracy only on the difference of angles $\varphi - \varphi_0$. This property is obviously inherent in the fields scattered by axisymmetric structures. However, it should be noted that the graphs in Fig. 7 were calculated for a strongly asymmetric shell.

3. QUASI-STATIC PLASMON RESONANCES IN THIN SHELLS

Let us define

$$l = b - a. \tag{11}$$

Below we assume the following conditions:

$$l \ll a \ll \lambda. \tag{12}$$

In this case, the thickness of the shell depends on the angle φ by the law

$$d(\varphi) = l - \delta\cos\varphi. \tag{13}$$

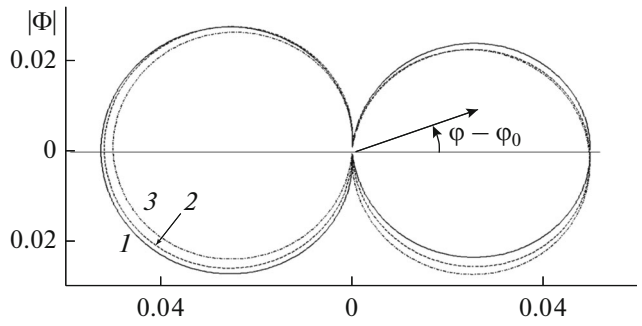

Fig. 7. The absolute values of the far-field patterns of a shell for $a = 18$ nm, $b = 20$ nm, $\delta = 1.9$ nm, $\lambda = 810$ nm, and $\varphi_0 = (1)\ 0$, $(2)\ \pi/4$, and $(3)\ \pi/2$.

The permittivity of gold satisfies the condition $|\varepsilon| \gg 1$. Therefore, the shell may be replaced with an infinitely thin film with a surface conductivity σ [8]:

$$\sigma = ikd\varepsilon/\eta. \tag{14}$$

The surface conductivity relates the tangential components of the electric and magnetic fields on the boundary $r = a$ by the formula

$$H_z(a-0,\varphi) - H_z(a+0,\varphi) = \eta\sigma E_\varphi(a,\varphi). \tag{15}$$

Taking into account (13), we write formula (14) as

$$\eta\sigma = -ik\alpha(1-\beta\cos\varphi), \tag{16}$$

where

$$\alpha = -\varepsilon l, \tag{17}$$

$$\beta = \delta/l. \tag{18}$$

Thus, a thin metal shell may be replaced with an infinitely thin film whose conductivity (16) is characterized by two parameters: α and β. If we neglect the heat loss in gold ($\varepsilon'' = 0$), then α will be a real positive quantity and, with allowance for the loss, $\alpha = \alpha' + i\alpha''$, $\alpha'' \ll \alpha'$.

Let us study the quasi-static oscillations of a quartz cylinder of radius a, covered with an infinitely thin layer of a material with a conductivity depending on the angle φ by formula (16).

Inside the cylinder and in its static near zone, $(kr \ll 1)$ the wave field $U(r,\varphi)$ approximately satisfies Laplace's equation

$$\frac{\partial^2 U}{\partial r^2} + \frac{1}{r}\frac{\partial U}{\partial r} + \frac{1}{r^2}\frac{\partial^2 U}{\partial \varphi^2} = 0. \tag{19}$$

The boundary conditions on the cylinder surface $r = a$ have the form

$$\frac{1}{\varepsilon_{qz}}\frac{\partial U}{\partial r}(a-0,\varphi) = \frac{\partial U}{\partial r}(a+0,\varphi), \tag{20}$$

$$U(a-0,\varphi) - U(a+0,\varphi) = \alpha(1-\beta\cos\varphi)\frac{\partial U}{\partial r}(a+0,\varphi). \tag{21}$$

We will seek partial solutions of problem (19)–(21) that decrease as $r \to \infty$. Since the problem is homogeneous, its nontrivial solutions exist only at definite values of the parameter α. These discrete values α_m are eigenvalues of the boundary value problem.

Let us show that the eigenfunctions $U_m(r,\varphi)$ and eigenvalues α_m are described by simple analytical expressions. Define two real positive parameters $t_1 > a$ and $t_2 < a$:

$$t_{1,2} = a\frac{1 \pm \sqrt{1-\beta^2}}{\beta}. \tag{22}$$

The values of t_1 and t_2 satisfy the relationships

$$t_1 + t_2 = \frac{2a}{\beta},\quad t_1 - t_2 = \frac{2a\sqrt{1-\beta^2}}{\beta},\quad t_1 t_2 = a^2. \tag{23}$$

The wave fields and the corresponding eigenvalues α_m are expressed by the formulas

$$U_m(r,\varphi) = \begin{cases} 1 + \varepsilon_{qz}\left(\dfrac{t_1}{t_2}\right)^m \left(\dfrac{r\exp(i\varphi) - t_2}{r\exp(i\varphi) - t_1}\right)^m, \\ r < a, \\ 1 - \left(\dfrac{r\exp(-i\varphi) - t_1}{r\exp(-i\varphi) - t_2}\right)^m, \quad r > a, \end{cases} \tag{24}$$

$$\alpha_m = \frac{(\varepsilon_{qz}+1)a}{m\sqrt{1-\beta^2}}, \tag{25}$$

where $m = 1,2,3\ldots$.

Fields (24) satisfy Laplace's equation (19), because they are analytic functions of the complex variables $r\exp(i\varphi)$ or $r\exp(-i\varphi)$. The requirement for the parameter m to be integer and positive is necessary for the absence of singularities of the corresponding functions of complex variable at the points $r = t_1$, $\varphi = 0$ and $r = t_2$, $\varphi = 0$. Boundary conditions (20) and (21) are easily tested directly. In this case, it is necessary to use formulas (23) and (25) and the relationship

$$1 - \beta\cos\varphi = -\frac{\beta}{2a^2}(a\exp(-i\varphi) - t_1) \times (a\exp(-i\varphi) - t_2)\exp(i\varphi) = -\frac{\beta}{2a^2}(a\exp(i\varphi) - t_1)(a\exp(i\varphi) - t_2)\exp(-i\varphi), \tag{26}$$

which follows from (23).

The asymptotics of the functions $U_m(r,\varphi)$ as $r \gg t_1$ has the form

$$U_m(r,\varphi) \sim m\frac{t_1 - t_2}{r}\exp(i\varphi). \tag{27}$$

Continuing quasi-static near field (27) to the far zone with the help of the function $H_1^{(2)}(kr)$, we obtain the far-field pattern of this field:

$$\Phi_m(\varphi) = \frac{\pi k}{2} m(t_1 - t_2)\exp(i\varphi). \tag{28}$$

The functions $U_m(r,\varphi)$ are complex, and the corresponding eigenvalues α_m prove to be real. This means that the complex-conjugate functions $U_m^*(r,\varphi)$ also satisfy the boundary conditions of the problem. Thus, in the quasi-static approximation, two-fold degeneracy in the structure under consideration takes place.

Using (17) and (18), we can rewrite expression (25) in terms of the resonance values of the permittivity of the shell:

$$\varepsilon_m = -\frac{\varepsilon_{qz}+1}{m}\frac{a}{\sqrt{l^2-\delta^2}},\ \ m=1,2,3\ldots \tag{29}$$

With variation in the frequency of optical oscillations, the complex permittivity of gold can approach the value of ε_m. At these frequencies, the field in the diffraction problem must have resonance bursts. For the structure with the spectrum represented by curve *2* in Fig. 6, from formula (29), we obtain $\varepsilon_1 \approx -32$, $\varepsilon_2 \approx -16$. As follows from Fig. 2, these values correspond to wavelengths conforming to the positions of the resonances in curve *2*.

4. ANALYTICAL SOLUTION OF THE DIFFRACTION PROBLEM IN THE QUASI-STATIC APPROXIMATION

According to the generalized method of eigenoscillations [9], the field $U(r,\varphi)$ in the diffraction problem can be represented by an expansion in the functions $U_m(r,\varphi)$ and $U_m^*(r,\varphi)$. The eigenfunctions $U_m(r,\varphi)$ satisfy Laplace's equation (19) and the following boundary conditions:

$$\frac{1}{\varepsilon_{qz}}\frac{\partial U_m}{\partial r}(a-0,\varphi) = \frac{\partial U_m}{\partial r}(a+0,\varphi), \tag{30}$$

$$U_m(a-0,\varphi) - U_m(a+0,\varphi) = \alpha_m(1-\beta\cos\varphi)\frac{\partial U_m}{\partial r}(a+0,\varphi). \tag{31}$$

These boundary conditions differ from boundary conditions (20) and (21) for the sought field $U(r,\varphi)$ by the replacement of the parameter α with α_m. Conditions (30) and (31) also hold for the functions $U_m^*(r,\varphi)$.

We obtain the generalized oscillations by the so-called ρ-method, i.e., by introducing the eigenvalue into the true two-sided boundary conditions [9].

The total field is sought in the form of the expansion

$$U(r,\varphi) = \tilde{U}(r,\varphi) + \sum_{m=1}^{\infty}\left[A_m U_m(r,\varphi) + B_m U_m^*(r,\varphi)\right], \tag{32}$$

where $\tilde{U}(r,\varphi)$ is the quasi-static solution of the problem of diffraction of a plane wave (7) by a quartz filament without a conducting film. The field $\tilde{U}(r,\varphi)$ satisfies Laplace's equation and the following boundary conditions:

$$\frac{1}{\varepsilon_{qz}}\frac{\partial \tilde{U}}{\partial r}(a-0,\varphi) = \frac{\partial \tilde{U}}{\partial r}(a+0,\varphi), \tag{33}$$

$$\tilde{U}(a-0,\varphi) = \tilde{U}(a+0,\varphi). \tag{34}$$

Series (32) satisfies Eq. (19) and boundary condition (20) term-wise. Substituting representation (32) into boundary condition (21) and taking into account formulas (30), (31), (33), and (34), we obtain the relationship

$$\sum_{m=1}^{\infty}(\alpha_m-\alpha)\left[A_m\frac{\partial U_m}{\partial r}(a+0,\varphi) + B_m\frac{\partial U_m^*}{\partial r}(a+0,\varphi)\right] = \alpha\frac{\partial \tilde{U}}{\partial r}(a+0,\varphi), \tag{35}$$

from which, using the orthogonality of eigenoscillations, we will obtain explicit expressions for the coefficients A_m and B_m.

The quasi-static field near the circular dielectric cylinder is known:

$$\tilde{U}(r,\varphi) = 1 - ikr\cos(\varphi-\varphi_0) - i\frac{\varepsilon_{qz}-1}{\varepsilon_{qz}+1}\frac{ka^2}{r}\cos(\varphi-\varphi_0),\ \ r>a. \tag{36}$$

The corresponding far-field pattern is expressed by the formula

$$\tilde{\Phi}(\varphi) = -i\frac{\pi}{2}\frac{\varepsilon_{qz}-1}{\varepsilon_{qz}+1}k^2a^2\cos(\varphi-\varphi_0). \tag{37}$$

Using formula (36), we find the right-hand side of relationship (35):

$$\frac{\partial \tilde{U}}{\partial r}(a+0,\varphi) = -\frac{2ik}{\varepsilon_{qz}+1}\cos(\varphi-\varphi_0). \tag{38}$$

We have the following conditions of orthogonality:

$$\int_0^{2\pi}(1-\beta\cos\varphi)\frac{\partial U_m}{\partial r}(a+0,\varphi)\frac{\partial U_n^*}{\partial r} \times (a+0,\varphi)d\varphi = \frac{\pi m^2\beta}{a^3}(t_1-t_2)\left(\frac{t_1}{t_2}\right)^m\delta_{mn}, \tag{39}$$

$$\int_0^{2\pi}(1-\beta\cos\varphi)\frac{\partial U_m}{\partial r}(a+0,\varphi)\frac{\partial U_n}{\partial r}(a+0,\varphi)d\varphi = 0, \tag{40}$$

where δ_{mn} is the Kronecker delta. To prove these relationships, it is necessary to use formula (26) and the expressions

$$\frac{\partial U_m}{\partial r}(a+0,\varphi) = -m(t_1-t_2) \times \left(\frac{t_1}{t_2}\right)^m \frac{(a\exp(i\varphi)-t_2)^{m-1}}{(a\exp(i\varphi)-t_1)^{m+1}}\exp(i\varphi), \quad (41)$$

$$\frac{\partial U_n^*}{\partial r}(a+0,\varphi) = -n(t_1-t_2) \times \frac{(a\exp(i\varphi)-t_1)^{n-1}}{(a\exp(i\varphi)-t_2)^{n+1}}\exp(i\varphi), \quad (42)$$

which follow from (24). The integration with respect to φ in (39) and (40) should be replaced with the integration in the complex plane of t over a closed circular contour $t = a\exp(i\varphi)$, and then we can find the residue of the integrated function at the pole $t = t_2$.

Using the orthogonality conditions (39) and (40), we can find from relationship (35) the coefficients A_m and B_m. For example, in order to determine A_m, we should multiply (35) by $(1-\beta\cos\varphi)\frac{\partial U_m^*}{\partial r}(a+0,\varphi)$ and integrate the results over the interval $(0, 2\pi)$. For calculating the right-hand side of the equality, we need the formula

$$\int_0^{2\pi} \frac{\partial U_m^*}{\partial r}(a+0,\varphi)(1-\beta\cos\varphi)\cos(\varphi-\varphi_0)d\varphi = -\frac{\pi\beta m^2}{2a^3}(t_1-t_2)^2\exp(-i\varphi_0). \quad (43)$$

As a result, we find the coefficients A_m and B_m in the form

$$A_m = \frac{\alpha}{\alpha_m - \alpha\varepsilon_{qz}+1}\frac{ik}{}(t_1-t_2)\left(\frac{t_2}{t_1}\right)^m\exp(-i\varphi_0), \quad (44)$$

$$B_m = \frac{\alpha}{\alpha_m - \alpha\varepsilon_{qz}+1}\frac{ik}{}(t_1-t_2)\left(\frac{t_2}{t_1}\right)^m\exp(i\varphi_0). \quad (45)$$

Separate terms in the expansion of the near field (32) correspond to the far fields whose patterns are determined by expressions (28) and (37). Therefore, we express the far-field pattern $\Phi(\varphi)$ and the total scattering cross section σ_s as follows:

$$\Phi(\varphi) = -i\frac{\pi k^2 a^2}{2(\varepsilon_{qz}+1)}\left[\varepsilon_{qz}-1+2\alpha\frac{(t_1-t_2)^2}{a^2} \times \sum_{m=1}^{\infty}\frac{m}{\alpha-\alpha_m}\left(\frac{t_2}{t_1}\right)^m\right]\cos(\varphi-\varphi_0), \quad (46)$$

$$k\sigma_s = \frac{\pi^2 k^4 a^4}{2(\varepsilon_{qz}+1)^2}\left|\varepsilon_{qz}-1+2\alpha\frac{(t_1-t_2)^2}{a^2} \times \sum_{m=1}^{\infty}\frac{m}{\alpha-\alpha_m}\left(\frac{t_2}{t_1}\right)^m\right|^2. \quad (47)$$

It should be noted that the far-field pattern (46) depends only on the difference of the angles $\varphi-\varphi_0$, which is a property of axisymmetric scatterers, to which the structure under consideration does not belong

From formulas (10) and (21), we obtain the following expressions:

$$k\sigma_a = \frac{a\alpha''}{|\alpha|^2}\int_0^{2\pi}|U(a-0,\varphi)-U(a+0,\varphi)|^2\frac{d\varphi}{1-\beta\cos\varphi}. \quad (48)$$

Substituting expansion (32) into (48) and transforming it with the help of formulas (25), (31), (39), (40), (44), and (45), we obtain

$$k\sigma_a = \frac{4\pi k^2 a\alpha''(t_1-t_2)^2}{\sqrt{1-\beta^2}}\sum_{m=1}^{\infty}\frac{1}{|\alpha-\alpha_m|^2}\left(\frac{t_2}{t_1}\right)^m. \quad (49)$$

It turned out that the absorption cross section, as well as the scattering cross section, is independent of the incidence angle φ_0.

Figure 8a shows the dependences—calculated according to (47)—of the total scattering cross section σ_s on the wavelength λ for the structure with the parameters $b = 20$ nm, $a = 18$ nm , and $\delta = 0$, 1, and 1.5 nm. Curves in Fig. 8a agree well with the results of rigorous calculations presented in Fig. 6.

With the help of calculations by formula (49), we obtained the scattering cross section σ_a as a function of the wavelength λ (Fig. 8b). The parameters of the structure are the same as for Fig. 8a. From the comparison of Figs. 8a and 8b, it follows that higher order plasmon resonances ($m = 2,3\ldots$) manifest themselves more strongly in the absorption spectrum.

The scattering and absorption cross sections of a coaxial shell can be found from expansions (47) and (49) by passing to the limit $\beta \to 0$, $t_1 \to \infty$, $t_2 \to 0$. In this case, only the terms with $m = 1$ are nonzero. As a result, we obtain

$$k\sigma_s = \frac{\pi^2 k^4 a^4}{2}\left|\frac{\alpha-(\varepsilon_{qz}-1)a}{\alpha-(\varepsilon_{qz}+1)a}\right|^2, \quad (50)$$

$$k\sigma_a = \frac{4\pi k^2 a^3\alpha''}{|\alpha-(\varepsilon_{qz}+1)a|^2}. \quad (51)$$

Finally, let us turn to the effect of a significant reduction on the visibility of such a structure, which can be explained by means of formula (50). The results

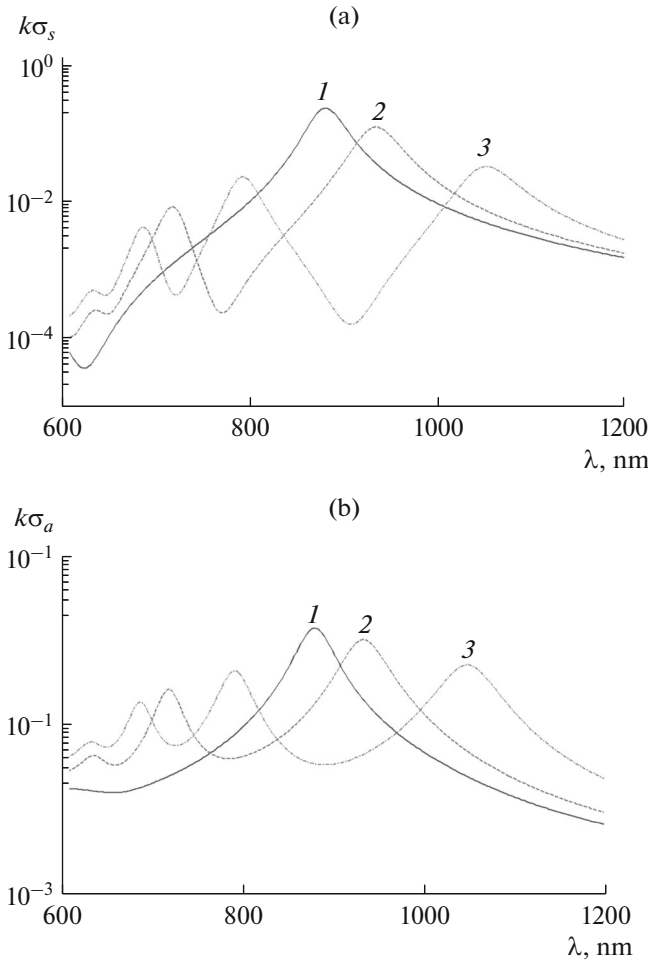

Fig. 8. The (a) total scattering and (b) absorption cross sections vs. the wavelength for $a = 18$ nm, $b = 20$ nm, $\varphi_0 = 0$, and $\delta = (1)$ 0, (2) 1, and (3) 1.5 nm.

of rigorous numerical calculation of the scattering spectrum of a coaxial shell with the parameters $a = 18$ nm and $l = 2$ nm have been presented above (Fig. 6, curve *1*). Note a deep dip of curve *1* at the wavelength $\lambda \approx 620$ nm, where the total cross section attains the value of $k\sigma_s \sim 4 \times 10^{-5}$. The power scattered by the quartz filament without coating is greater by an order of magnitude: $k\sigma_s \sim 7 \times 10^{-4}$. Thus, we have an effect of a substantial reduction in the visibility of a filament after depositing on it a thin metal layer [3]. According to formula (50), the minimum value of $k\sigma_s$ is reached on satisfying the condition $\alpha' = (\varepsilon_{qz} - 1)a$, i.e., at $\varepsilon' = -(\varepsilon_{qz} - 1)\,a/l \approx -10$. As follows from the analysis of Fig. 2, this value of ε' corresponds to the wavelength of the dip.

CONCLUSIONS

The problem of diffraction of a plane wave on a noncoaxial cylindrical gold shell has been considered for the case of TM-polarization. The influence of the distance between the centers of the cylindrical boundaries on the spectral characteristics of the scattered field has been studied by rigorous numerical methods. It has been found that, with increasing distance between the centers of the cylindrical boundaries of the shell, the number of plasmon resonances increases. For thin shells, an approximate quasi-static theory based on the replacement of the shell by a film with a variable conductivity has been developed. Analytical expressions for plasmon resonance frequencies and scattering and absorption spectra have been obtained. It has been shown that, within its range of applicability, the results of the approximate theory are in a good agreement with rigorous numerical results.

ACKNOWLEDGMENTS

This work was supported in part by the Russian Foundation for Basic Research, project no. 16-02-00247-a.

REFERENCES

1. V. V. Klimov, *Nanoplasmonics* (Fizmatlit, Moscow, 2009) [in Russian].
2. E. A. Velichko and A. I. Nosich, Opt. Lett. **38**, 4978 (2013).
3. A. P. Anyutin, I. P. Korshunov, and A. D. Shatrov, J. Commun. Technol. Electron. **60**, 952 (2015).
4. P. B. Johnson and R. W. Christy, Phys. Rev. B **6**, 4370 (1972).
5. A. G. Kyurkchan, S. A. Minaev, and A. L. Soloveichik, J. Commun. Technol. Electron. **46**, 615 (2001).
6. A. P. Anyutin and V. I. Stasevich, J. Quant. Spectr. Radiation Transfer **100** (1–3), 16 (2006).
7. A. G. Kyurkchan and N. I. Smirnova, *Mathematical Modeling in Diffraction Theory with A Priori Information on Analytic Properties of the Solution* (ID Media Publisher, Moscow, 2014) [in Russian].
8. S. M. Apollonskii and V. T. Erofeenko, *Electromagnetic Fields in Screening Shells* (Minsk. Univ., Minsk, 1988) [in Russian].
9. N. N. Voitovich, B. Z. Katsenelenbaum, and A. N. Sivov, *A Generalized Eigenmode Method in the Diffraction Theory* (Nauka, Moscow, 1977) [in Russian].

Translated by E. Chernokozhin